Electronic Supplementary Information

Anionic Metal-Organic Frameworks Lead the Way to Eco-Friendly High-Energy-Density Materials

Yongan Feng, [a] Yangang Bi [‡, b], Wenyuan Zhao [‡, a] and Tonglai Zhang [*, a]

[a] State Key Laboratory of Explosion Science and Technology, Ministry of Science and Technology of China, School of Mechatronical Engineering, Beijing Institute of Technology, 5 South Zhongguancun Street, Beijing 100081, P. R. China

[b] Key Laboratory of Polymer Chemistry and Physics of the Ministry of Education of China, Department of Polymer Science and Engineering, College of Chemistry and Molecular Engineering, Peking University, 5 Yiheyuan Road, Beijing 100871, P. R. China

[‡] These authors contributed equally to this work

* Corresponding Author: Prof. Tonglai Zhang

Email:

Tonglai Zhang: ztlbit@bit.edu.cn

Yongan Feng: fengyongan0918@126.com

Table of contents

1. Materials and instruments

All the materials and chemical reagents with analytical grade were bought from the reagents company (Aladdin) and used without further purification. IR spectra of ligand was measured on a Bruker Equinox 55 infrared spectrometer by using KBr pellets from 400 to 4000 cm^{-1} with a resolution of 4 cm^{-1}. Elemental analyses (C, H and N) were performed on a Flash EA 1112 fully automatic trace element analyzer. The purities of the bulk samples were verified by X-ray powder diffraction (XRPD) measurements performed on a Bruker D8 advance diffractometer at 60 kV, 300 mA and Cu Kα radiation (λ=1.5406 Å), with a scan speed of 5°·min^{-1} and a step size of 0.02° in 2θ. The single crystal X-ray diffraction data collections were carried out on a Rigaku AFC-10/Saturn 724+CCD diffractometer with graphite-monochromated Mo Kα radiation (λ=0.71073 Å) using the multi-scan technique. The structures were determinedby direct methods using SHELXS-97[1] and refined by full-matrix least-squares procedures on F_2 with SHELXL-97.[2] All non-hydrogen atoms were obtained from the difference Fourier map and subjected to anisotropic refinement by full-matrix least squares on F_2. Hydrogen atoms were obtained geometrically and treated as riding on the parent atoms or were constrained in the locations during refinements. Thermal stability measurements were performed/tested/analyzed by using differential scanning calorimetry (DSC) on a CDR-4 of Shanghai Precision & Scientific Instrument Co., Ltd. at a heating rate of 5°C min^{-1} from 50°C to 500°C. Thermogravimetric analyses (TG) were operated on a Netzsch STA 449C instrument at a heating rate of 5°C min^{-1} from 50°C to 600°C under dry oxygen-free nitrogen atmosphere with a flowing rate of 20 mL min^{-1}. Impact sensitivities were tested by fall hammer apparatus applying standard staircase method using a 2 kg drop weight and the results were reported in terms of height for 50% probability of explosion ($h_{50\%}$).[3] The friction sensitivities were measured on a Julius Peter's apparatus by following the BAM method. The electrostatic sensitivities were analyzed by using JGY-50(III) Electrostatic test apparatus.[4]

2. Synthetic procedures

Caution! Although no accidents occurred during the synthesis and handling of the materials discussed in this work, these compounds are high-energy materials and tend to explode under certain conditions. All of the complexes should be treated with discretion and appropriate safety precautions must be taken at all times. Bis(tetrazole) methane(H2btm) was synthesized by using an improved greener preparation method based on Sherpless method in order to expand production capacity and reduce the cost.

Bis(tetrazole)methane (H2btm). Malononitrile (97mmol, 6.407g), sodium azide (232.8mmol, 15.137g), and zinc chloride (194mmol，26.442g) were suspended in water (400 mL) and the mixture reacted under reflux for 12h. After cooling to room temperature, NaOH (15.52g, 100mL) was added to form the precipitation of zinc hydroxide. The filtrate was collected by filtration and acidized with concentrated HCl (57.35g, 100mL). After evaporation, water was removed. The remaining solid was extracted by boiling isopropyl alcohol. H2btm was obtained by removing isopropyl alcohol, 89% yield. This reaction can be scaled up to larger amounts. Tm=214.9°C. 1H NMR (400 MHz, [D_6] DMSO, ppm): 4.75 (2H, s, CH_2CN_4H); 15.55(2H, br. s, CN_4H). IR (cm^{-1}, KBr): 3200, 2800, 1567, 1452, 1432, 1405, 1273, 1242, 1197, 1105, 1076. Elemental analysis (%) for $C_3H_4N_8$ (152.12): C, 23.69; H, 2.65; N, 73.66; found: C, 23.57; H, 2.59; N, 73.58%.

$(AG)_3(Co(btm)_3)$ (1). A mixture of H2btm (0.456g, 3mmol) and NaOH (0.24g, 6mmol) were dissolved in 10 mL of water and stirred at 70 °C for 10 min to form a faint yellow solution. Then aminoguanidine hydrochloride (0.663g, 6mmol) in 5 mL water was added to the above-mentioned solution.Then the mixture was stirred at 70 °C for 20 min. $CoCl_2·6H_2O$ (0.238 g, 1 mmol) was dropped gradually to the solution, and immediately the fresh pink precipitation was produced. About 10 min later, the precipitation disappeared and formed orange clear solution. The clear solution was cooled down to room temperature. After filtration, the crystals suitable for single-crystal X-ray diffraction measurement were obtained by slow crystallization from water (Yield 89%). Elemental analysis (%) for $C_{12}H_{27}N_{36}Co_1$ (734.52): C, 19.62; H, 3.71; N, 68.65. Found: C, 19.58; H, 3.66; N, 68.61%. The XPS spectrum of the crystalline sample shows evident satellite peaks of 780eV, suggesting Co (III) in compound **1**.

$\{(AG)_2[Cu(btm)_2]\}_n$ (2). The synthesis method for compound **2** was similar to that of **1** except that 1 mmol of $CuCl_2·2H_2O$ was used instead of 1 mmol of $CoCl_2·6H_2O$. The crystals suitable for single-crystal X-ray diffraction measurements were obtained by slow crystallization from water (Yield 86%). Elemental analysis (%) for $C_8H_{18}N_{24}Cu_1$ (513.94): C, 18.69; H, 3.53; N, 65.41. Found: C, 18.62; H, 3.47; N, 65.34. The XPS spectrum of the crystalline sample shows evident satellite peaks of 933eV, suggesting Cu (II) in compound **2**.

3. X-ray powder diffraction (XRPD)

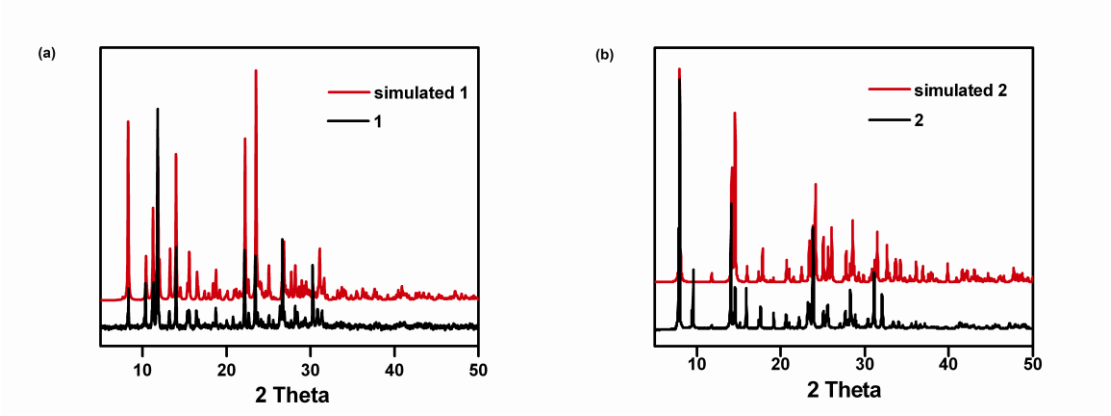

Figure S1. (Left) X-ray powder diffraction (XRPD) curve of compound **1**. (Right) XRPD curve of compound **2**.

4. X-ray crystallography determinations

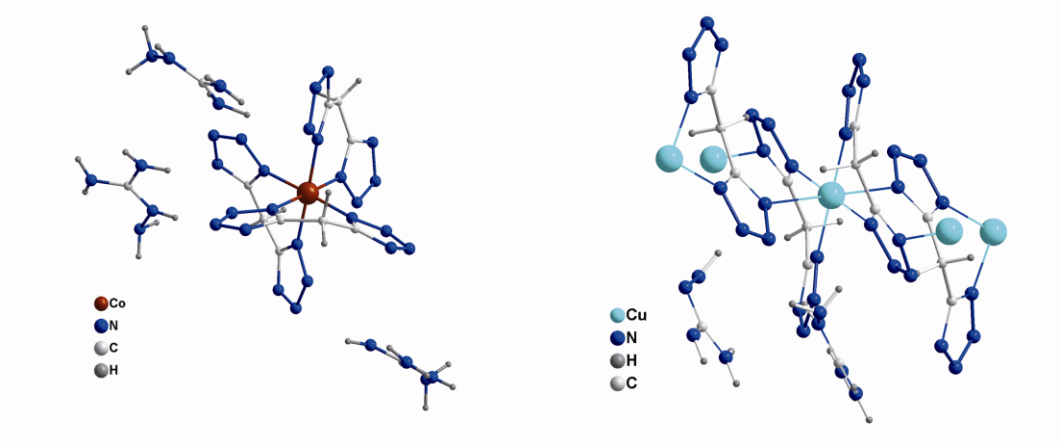

Figure S2. (Left) Molecule structure of compound **1.** (Right) Molecule structure of compound **2**.

Table S1. Crystal data and structure refinement details for the two complexes.

Item	**1**	**2**
CCDC	1449926	1449928
Empirical formula	$CoC_{12}H_{27}N_{36}$	$CuC_8H_{18}N_{24}$
Formula weight	734.63	514
Temperature/K	153(2)	101.8
Crystal system	monoclinic	monoclinic
Space group	P_{21}/c	P_{21}/c
a/Å	10.859(2)	11.590(5)
b/Å	15.719(3)	10.2064(5)
c/Å	17.294(3)	8.269(4)
α/°	90	90

β/°	100.957(3)	107.10(5)
γ/°	90	90
Volume/Å^3	2898.3(10)	934.9(6)
Z	4	2
P_{calc}/g cm^{-3}	1.684	1.826
μ/mm^{-1}	0.672	1.231
F(000)	1512	526
Crystal size/mm^3	0.47 × 0.33 × 0.22	0.50 × 0.50 × 0.45
Radiation	MoKα (λ = 0.7107)	Mo Kα (λ = 0.7107)
2Θ range for data collection/°	4.62 to 58.26	6.7 to 51.94
Reflections collected	25540	3797
Independent reflections	7745	1833
Data/restraints/parameters	7745/0/527	1833/0/151
Goodness-of-fit on F2	1.002	1.091
Final R indexes [I>=2σ (I)]	R1 = 0.0547	R1 = 0.0293
Final R indexes [I>=2σ (I)]	wR2 = 0.1511	wR2 = 0.0663
Final R indexes [all data]	R1 = 0.0619	R1 = 0.0333
Final R indexes [all data]	wR2 = 0.1593	wR2 = 0.0680
Largest diff. peak/hole/e Å^{-3}	0.51/-0.71	0.33/-0.35

Table S2. Selected bond lengths (Å) and bond angles (°) for the complexes.

Compound 1			
Item	Bond lengths	Item	Bond angles
Co(1)-N(17)	1.9112(18)	N(1)-Co(1)-N(16)	178.58(7)
Co(1)-N(1)	1.9192(19)	N(8)-Co(1)-N(24)	178.14(8)
Co(1)-N(24)	1.9233(18)	N(9)-Co(1)-N(17)	178.11(8)
Co(1)-N(16)	1.9312(19)	N(1)-Co(1)-N(8)	88.63(8)
Co(1)-N(9)	1.9344(19)	N(8)-Co(1)-N(16)	92.78(8)
Co(1)-N(8)	1.9358(18)	N(1)-Co(1)-N(9)	92.04(8)
Compound 2			
Item	Bond lengths	Item	Bond angles
Cu(1)-N(1)	2.0229(17)	N(1)-Cu(1)-N(1')	180.00(7)
Cu(1)-N(1')	2.0229(17)	N(5')-Cu(1)-N(1')	85.29(7)

Cu(1)-N(4)	2.535	N(5)-Cu(1)-N(1')	94.71(7)
Cu(1)-N(4')	2.535	N(5)-Cu(1)-N(1)	85.29(7)
Cu(1)-N(5)	2.0084(19)	N(5')-Cu(1)-N(1)	94.71(7)
Cu(1)-N(5')	2.0084(19)	N(5)-Cu(1)-N(5')	180.0

5. Hydrogen bond

Due to 29 different connection atoms combinations, there are 29 different kinds of H-bonds in Compound **1**. Each connection atoms combination corresponds to only one kind of H-bond. Likewise, 12 different kinds of H-bonds exist in compound 2. Detailed information is shown in the table below.

Table S3. Selected bond lengths (Å) and bond angles (°) for the complexes.

Compound 1				
A—H···B	A—H (Å)	H···B (Å)	A···B (Å)	Angles (°)
N(25) —H(25A)···N(23)	0.9700	2.2800	3.1885	155.00
N(25) —H(25B)···N(3)	0.9600	2.2300	3.1495	160.00
N(26) —H(26)···N(5)	0.82	2.1700	2.9898	175.00
N(27) —H(27A)···N(4)	0.8800	2.2200	3.0719	163.00
N(27) —H(27B)···N(6)	0.8500	2.3200	3.1421	163.00
N(28) —H(28A)···N(25)	0.8500	2.2600	2.6690	109.00
N(28) —H(28B)···N(13)	0.8900	2.3300	3.0933	144.00
N(29) —H(29A)···N(7)	0.9100	2.2900	3.0575	141.00
N(29) —H(29B)···N(19)	0.9100	2.1000	2.9663	159.00
N(30) —H(30)···N(21)	0.9000	2.0800	2.9747	168.00
N(31) —H(31A)···N(14)	0.8300	2.1200	2.9043	158.00
N(31) —H(31B)···N(21)	0.9000	2.6100	3.3049	135.00
N(31) —H(31B)···N(22)	0.9000	2.0900	2.9585	163.00
N(32) —H(32A)···N(10)	0.9800	2.1700	3.1112	161.00
N(32) —H(32A)···N(11)	0.9800	2.4400	3.2258	137.00
N(32) —H(32B)···N(29)	0.9000	2.2600	2.6513	106.00
N(33) —H(33A)···N(20)	0.8900	2.4800	3.1993	138.00
N(33) —H(33B)···N(11)	0.9200	2.2300	3.1065	161.00
N(33) —H(33B)···N(12)	0.9200	2.5200	3.1719	129.00
N(34) —H(34)···N(2)	0.8800	2.3300	3.1628	159.00
N(35) —H(35A)···N(7)	0.8100	2.2600	3.0716	173.00
N(35) —H(35B)···N(2)	0.9300	2.5300	3.3560	149.00

N(35) —H(35B)---N(3)	0.9300	2.4800	3.2747	144.00
N(36) —H(36A)---N(15)	0.8600	2.2100	3.0160	155.00
N(36) —H(36B)---N(33)	0.8300	2.3500	2.7061	107.00
N(36) —H(36B)---N(33)	0.8300	2.4300	3.1332	143.00
C(2) —H(2B)---N(13)	0.9900	2.6000	3.2657	124.00
C(8) —H(8A)---N(11)	0.9900	2.4300	3.2081	135.00
C(8) —H(8B)---N(20)	0.9900	2.5700	3.5292	164.00
Compound 2				
A—H---B	A---H (Å)	H---B (Å)	A---B (Å)	Angles (°)
N(9) —H(9A)---N(7)	0.8800	2.1200	2.9578	160.00
N(9) —H(9B)---N(6)	0.8800	2.0600	2.9380	171.00
N(9) —H(9B)---N(7)	0.8800	2.5000	3.2934	150.00
N(10) —H(10A)---N(8)	0.8800	2.2600	3.1111	163.00
N(10) —H(10B)---N(12)	0.8800	2.3300	2.6655	103.00
N(10) —H(10B)---N(7)	0.8800	2.5700	3.2580	136.00
N(11) —H(11)---N(3)	0.8800	2.1200	2.8818	144.00
N(12) —H(12B)---N(4)	0.8700	2.6000	3.3002	138.00
C(1) —H(1B)---N(2)	0.9900	2.4900	3.3024	139.00
N(12) —H(12A)---N(9)	0.8000	2.2700	2.6707	111.00
N(12) —H(12B)---N(3)	0.8500	2.5500	3.2451	140.00
N(12) —H(12B)---N(4)	0.8500	2.3000	3.1314	169.00

6. Thermo-stability measurement (DSC and TG)

To investigate the thermal behavior of compound 1 and 2, DSC and TG-DTG of two compounds are tested with a linear heating rate of 5°C min^{-1} in flowing N_2 (flow rate 20mL min^{-1}). The curves are shown in figure S3 and S4.

In the DSC curve of compound **1**, a melting point peak came out/appeared at268.1 °C, then a Intense endothermic process can be seen at 285.5-312.2 °C. TG-DTG curves showed that the first mass loss occurred very rapidly and the percentage of total mass loss was 39.6%. The second exothermic decomposition stage was seen in the DSC curve between 312.2-384.8 °C and a peak was observed at 346.5 °C. The TG curve showed the mass loss of 17.6% in the second stage of decomposition. The third exothermic peak can be seen at 411 °C in the DSC curve. Residue mass accounted percentage of 24.9%, which is in good agreement with the calculated value of Co and C (27.6%) . It is within margin of error.

In the DSC curve of compound **2**, a melting point peak appeared at 212.5 °C, then two intense endothermic peaks can be seen at 248.6 and 393.7 °C, respectively. TG-DTG curves showed that the first

mass loss occurred very rapidly and the percentage of total mass loss was 50.1%, indicating that Cu-based energetic materials equipmore intense decomposition process than that of Co-based. The second exothermic decomposition stage was seen in the DSC curve after 335.6 °C and a peak was observed at 393.7 °C. The TG curve showed the mass loss is 37.3% in the second stage of decomposition. The final product percentage of 12.7% is in good agreement with the calculated value of Cu (12.4%), indicating that Cu-based anionic MOFs have great potential for eco-friendly energetic materials.

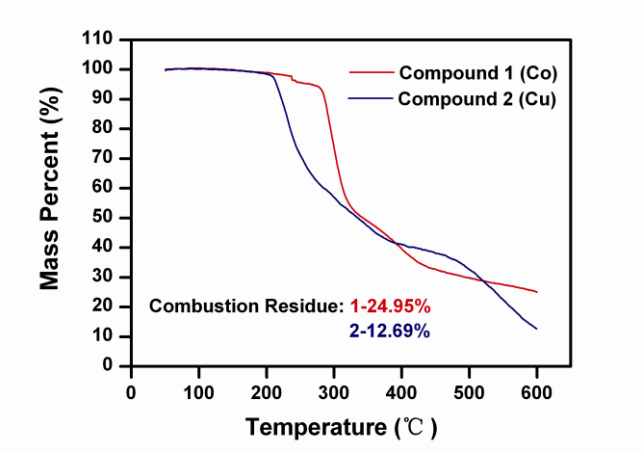

Figure S3. TG spectrums of compounds **1** and **2**.

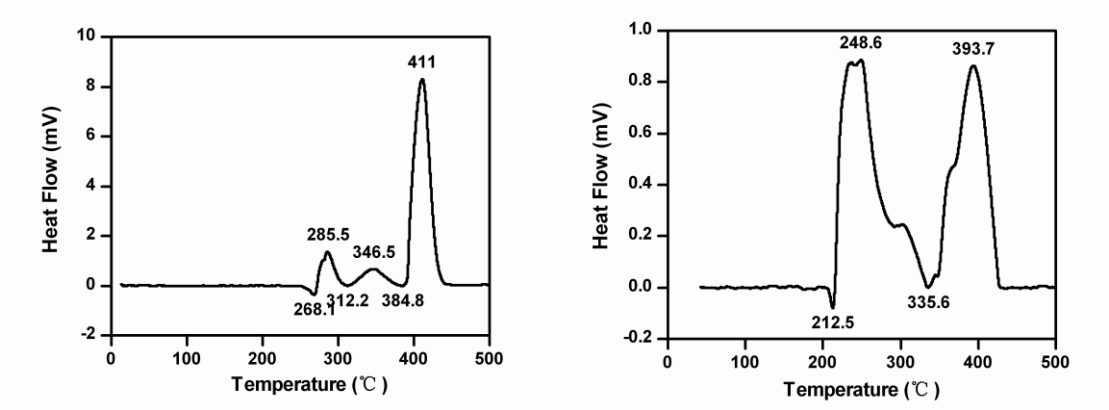

Figure S4. (Left) DSC spectrum of compound **1**. (Right) DSC spectrum of compound **2**.

7. Non-isothermal kinetics analysis

Kinetics parameters, including apparent activation energy (E_a) and the pre-exponential factor (A), were calculated by using Kissinger's method[5] (Eq. (1)) and Ozawa-Doyle's method[6] (Eq. (2)) according to the peak temperatures of first decomposition processes shown in the DSC curves.

$$\ln\frac{\beta}{T_p^2} = \ln\left(\frac{AR}{E_a}\right) - \frac{E_a}{RT_p} \quad (1)$$

$$\lg\beta + 0.4567\frac{E_a}{RT_p} = C \quad (2)$$

Where T_p is the peak temperature (°C) of first reaction process, A is the pre-exponential factor (s^{-1}), E_a is the apparent activation energy (kJ mol^{-1}), R is the gas constant (J mol^{-1} °C^{-1}), β is the heating rate (°C

min^{-1}) and C is a constant. The results are listed in table S4. The symbol "r" stands for the standard deviation. E_a is equal to the average of E_k and E_o.

Table S4. Peak temperature and kinetics parameters of **1** and **2**.

β (℃ min^{-1})	Peaks temperatures T_p (℃)	
	1	2
5	268.1	212.5
10	277.2	218.8
15	281.5	224.0
20	285.7	226.3
Kissinger's method		
E_k (kJ mol^{-1})	191.1	203.5
Log A (s^{-1})	16.26	19.8
Linear correlation coefficient (R_k)	-0.9988	-0.9941
r	3.393e-002	7.678e-002
Ozawa-Doyle's method		
E_o (kJ mol^{-1})	190.5	201.3
Linear correlation coefficient (R_k)	-0.9989	-0.9946
r	1.475e-002	3.332e-002
E_a (kJ mol^{-1})	190.8	202.4

8. Sensitivity

Impact sensitivity (IS) was determined by a fall hammer apparatus according to the China National Military Standard. Compound (20mg) is compacted to a copper cap under the press of 39.2 MPa and is hit by 2 kg drop hammer.

Friction sensitivities (FS) of three complexes are measured by applying a Julius Peter's machine using 20 mg sample.

Electrostatic sensitivities (EDS) are tested by using an ESD JGY-50 III Electrostatic test apparatus at 15 kV and 0.22 μF. Test conditions: 25°C (temperature); 32% (relative humidity).

Table S5. The sensitivities of title energetic MOFs **1** and **2**.

Compound	IS (J)	FS (N)	EDS (J)
1	>40	>360	>20
2	>40	>360	>20

9. Thermodynamic calculation

Energies of combustion (Δ_cH°) and Energies of formation (Δ_fH°) are two important parameters to assess the energetic properties of target compounds. They are calculated based on measurements of constant volume combustion energy (Δ_cU°). The experimental results for Δ_cU° of compounds **1** and **2** are shown in

the following table (Table S6). The standard molar enthalpy of combustion (Δ_cH°) can be obtained according to the formula (Eq. (3)).

$$\Delta_cH^\circ = \Delta_cU^\circ + \Delta nRT \quad (3)$$

Where $\Delta n = \Delta n_i$ (products, g) - Δn_j (reactants, g), Δn_i (mol) and Δn_j (mol) is the total molar amount of gases in the products and reactants, respectively. The enthalpies of formation (Δ_fH°, kJ mol^{-1}) at 298 K were calculated through the adoption of Hess thermochemical cycle on the basis of the combustion reactions (Eq. (4-5)). The heats of formation (Δ_fH) of the combustion products, CO_2(g) and H_2O (l), are -393.51 kJ mol^{-1} and -285.83 kJ mol^{-1}, respectively.

Compound 1 $$CoC_{12}H_{27}N_{36} + 19.25O_2 \rightarrow CoO + 12CO_2 + 13.5H_2O + 18N_2 \quad (4)$$

Compound 2 $$CuC_8H_{18}N_{24} + 13O_2 \rightarrow CuO + 8CO_2 + 9H_2O + 12N_2 \quad (5)$$

Table S6. Thermodynamic parameters of **1** and **2**.

Compounds	$\Delta_cU°$ (MJ Kg^{-1})	$\Delta_cU°$ (kJ mol^{-1})	$\Delta_cH°$ (kJ mol^{-1})	$\Delta_fH°$ (kJ mol^{-1})
1	12.8148	-9412.7089	-9338.3817	519.6567
2	13.0586	-6711.2886	-6661.7372	783.8872

10. Heat of detonation

The heats of detonation (ΔH_{det}) of compounds **1** and **2** were calculated using the method adopted by Hope-Weeks.[7] N_2, NH_3 and H_2O, except for metal-containing products, were treated as gas. Energies (E_f) of title materials compound 1 and 2 were computed by the Density functional theory (DFT) code $DMol_3$ under 3D periodic boundary conditions employing the Monkhorst Pack multiple K-point sampling of the Brillouin zone and the Perdew–Becke–Ezerhoff (PBE) exchange-correlation function. Energies of formation (ΔE_{det}) of the two compounds were calculated through the adoption of Hess thermochemical cycle on the basis of the detonation reactions (Eq. (6-8)).

$$\Delta E_{det} = \sum \Delta E_f(products) - \sum \Delta E_f(reactant) \quad (6)$$

Compound 1 $$CoC_{12}H_{27}N_{36} \rightarrow Co + 12C + 9NH_3 + 13.5N_2 \quad (7)$$

Compound 2 $$CuC_8H_{18}N_{24} \rightarrow Cu + 8C + 6NH_3 + 9N_2 \quad (8)$$

ΔH_{det} were estimated using a linear correlation equation (Eq. (9)) with a linearly dependent coefficient at 0.968, and listed in table S7.

$$\Delta H_{det} = 1.127\Delta._{det} + 0.046 \quad (9)$$

Table S7. Calculated parameters used in the detonation reactions for compounds **1** and **2**.

complex	E_f (hartree)	Metal	C	N_2	NH_3	ΔE_{det} (hartree)	ΔE_{det} (kcal g^{-1})	ΔH_{det} (kcal g^{-1})	ΔH_{det} (kcal cm^{-3})
1	-2588.8272	-145.0077	-37.738	-109.447	-56.5045	4.8885	4.1763	4.7527	8.0036
2	-1825.9680	-196.1132	-37.738	-109.447	-56.5045	3.9007	4.7628	5.4136	9.8853

11. Detonation performances

Detonation performances of the related energetic MOFs, including detonation velocity (D) and detonation pressure (P), were computed by the empirical Kamlet formula (Eq. (10-12)).

$$D = 1.01\Phi^{1/2}(1+1.30\rho) \quad (10)$$

$$P = 1.558\,\Phi\rho^2 \quad (11)$$

$$\Phi = 31.68N(MQ)^{1/2} \quad (12)$$

Where D is detonation velocity (km s^{-1}), P is detonation pressure (GPa), ρ is the density of explosive (g cm^{-3}), N is the moles of detonation gases per gram of explosive (mol g^{-1}), M is the average molecular weight of gaseous products (g mol^{-1}), Q is the heat of detonation (kcal g^{-1}). The detonation reactions are described as Equations (7) and (8).

Table S8. The calculation parameters of title energetic MOFs **1** and **2**.

Compound	N (mol g^{-1})	M (g mol^{-1})	Q (kcal g^{-1})	ρ (g cm^{-3})	D (km s^{-1})	P (GPa)
1	0.030	23.6	4.75	1.684	10.21	44.45
2	0.029	23.6	5.41	1.826	10.97	53.92

Here, Q is Heats of detonation (ΔH_{det}) mentioned in text.

Table S9. Physicochemical and energetic properties of **1** and **2**, along with those of some known high-performance energetic materials.

Compound	ρ[a]	N%[b]	T_d[c]	Q[d]	D[e]	P[f]	IS[g]	FS[h]
2	1.826	65.41	219	5.41	10.97	53.92	>40	>360
1	1.684	68.65	277	4.75	10.21	44.45	>40	>360
TRTR-3	2.44	49.1	355	3.96	10.4	56.5	32	>360
3-Atrz	1.83	51.68	285	3.63	8.75	34.3	>40	>360
ATRZ-1	1.68	53.35	243	3.62	9.16	35.68	22.5	>360
$[Co_9(bta)_{10}(Hbta)_2(H_2O)_{10}]_n$[8]	1.71	59.85	253	2.66	8.66	32.2	27	>360
$[Cu_4Na(Mtta)_5(CH_3CN)]_n$[9]	1.98	40.1	384	2.37	7.23	24.4	36	>360
$[Cu(Htztr)_2(H_2O)_2]_n$[10]	1.89	57.7	345	2.13	8.18	30.6	>40	>360
ATRZ-2	2.16	43.76	257	1.38	7.77	29.7	30	>360
NHP	1.98	33.49	220	1.37	9.18	39.69		
$[Pb(Htztr)_2(H_2O)]_n$[11]	2.52	39.4	340	1.36	7.72	31.6	>40	>360
$\{[Cu(tztr)]\cdot H_2O\}_n$[10]	2.32	45.2	325	1.32	7.92	32	>40	>360

CHP	1.95	14.71	194	1.25	8.23	31.73	5	
$[Ag(ntz)]_n$[12]	3.12	25.4	305	1.16	7.94	36.5	>40	>360
NHN [7,19]	2.16	40.14		1.04	7.30	20.2		
$[Ag(atz)]_n$[12]	2.97	29.3	348	0.78	6.52	24.1	>40	>360
CHHP	2	23.58	231	0.75	6.21	17.96	7.5	
ZHHP	2.12	23.61	293	0.7	7.02	23.58		
$[Pb(H_2tztr)(O)]_n$[11]	3.51	27.2	318	0.26	8.12	40.1	>40	>360
$[Co_9(bta)_{10}(Hbta)_2(H_2O)_{10}]_n \cdot (22\ H_2O)_n$[8]	1.96	51.78	300				>40	>360
$Cu(Mtta)_2(NO_3)_2$[13]	1.91	39.38	380				24.5	>360
Cu(3,5-DNBA)(N_3)[14]	2.03	22.1	275				23.5	>360
$[Cu_3(MA)_2(N_3]$[15]	2.09	47.55	178	2.47	8.47	35.32	>40	>360

H2bta=N,N-bis(1H-tetrazole-5-yl)-amine; Mtta=1-methyltetrazole or 5-methyltetrazole; H2tztr=3-(1H-tetrazol-5-yl)-1H-triazole ; Hatz =3-amine-1H-1,2,4-triazole ; Hntz = 3-nitro-1H-1,2,4-triazole; 3,5-DNBA=3,5-dinitrobenzoic acid; MA=melamine.

12. References

1 G. M. Sheldrick, SHELXS-97, Program for X-ray Crystal Structure Determination, University of Göttingen, Germany, 1997.
2 G. M. Sheldrick, SHELXL-97, Program for X-ray Crystal Structure Refinement, University of Göttingen, Germany, 1997.
3 R. Meyer and J. Köhler (Eds.), Explosives, 4th ed. revised and extended, VCH Publishers, New York, 1993, **149**.
4 R. Meyer and J. Köhler (Eds.), Explosives, 4th ed. revised and extended, VCH Publishers, New York, 1993, **197**.
5 H. E. Kissinger, *Anal. Chem.*, 1957, **29**, 1702-1706.
6 T. Ozawa, *Bull. Chem. Soc. Jpn.*, 1965, **38**, 1881-1886.
7 O. S. Bushuyev, B P. rown, A. Maiti, R. H. Gee, G. R. Peterson, B. L. Weeks, L. J. Hope-Weeks, *J. Am. Chem. Soc.*, 2012, **134**, 1422-1425.
8 S. Zhang, X. Liu, Q. Yang, Z. Su, W. Gao, Q. Wei, G. Xie, S. Chen, S. Gao, *Chem. Eur. J.*, 2014, **20**, 7906-7910.
9 Y. Feng, X. Liu, L. Duan, Q. Yang, Q. Wei, G. Xie, S. Chen, X. Yang, S. Gao, *Dalton Trans.*, 2015, **44**, 2333-2339.
10 X. Liu, W. Gao, P. Sun, Z. Su, S. Chen, Q. Wei, G. Xie, S. Gao, *Green Chem.*, 2015, **17**,831-836.
11 W. Gao, X. Liu, Z. Su, S. Zhang, Q. Yang, Q. Wei, S. Chen, G. Xie, X. Yang, S. Gao, *J. Mater. Chem. A*, 2014, **2**, 11958-11965.
12 X. Qu, S. Zhang, Q. Yang, Z. Su, Q. Wei, G. Xie, S. Chen, *New J. Chem.*, 2015, **39**, 7849-7857.
13 Q. Yang, S., G. Xie, S. Gao, *Journal of Hazardous Materials*, 2011, **197**, 199-203.
14 X. Liu, Q. Yang, Z. Su, S. Chen, G. Xie, Q. Wei, S. Gao, *RSC Adv.*, 2014, **4**, 16087-16093.
15 H. Zhang, M. Zhang, P. Lin, V. Malgras, J. Tang, S. M. Alshehri, Y. Yamauchi, S. Du, J. Zhang, *Chem. Eur.J.*, 2016, **22**, 1141-1145.